Global Biogeochemical Cycles

RESEARCH ARTICLE
10.1029/2018GB005921

Key Points:
- A survey of oceanographic conditions, as well as physical and geochemical properties of continental margin surface sediments, is presented
- Hydrodynamic processes on shallow continental shelves emerge as an important control on the ^{14}C contents of OC
- General characteristics of OC in global active and passive continental margin sediments are shown

Supporting Information:
- Supporting Information S1
- Table S1
- Data Set S1

Correspondence to:
R. Bao,
rui_bao@fas.harvard.edu

Citation:
Bao, R., van der Voort, T. S., Zhao, M., Guo, X., Montluçon, D. B., McIntyre, C., & Eglinton, T. I. (2018). Influence of hydrodynamic processes on the fate of sedimentary organic matter on continental margins. *Global Biogeochemical Cycles*, *32*, 1420–1432. https://doi.org/10.1029/2018GB005921

Received 6 MAR 2018
Accepted 4 SEP 2018
Accepted article online 20 SEP 2018
Published online 28 SEP 2018

Influence of Hydrodynamic Processes on the Fate of Sedimentary Organic Matter on Continental Margins

Rui Bao[1,2], Tessa S. van der Voort[1], Meixun Zhao[3,4], Xinyu Guo[5], Daniel B. Montluçon[1], Cameron McIntyre[1,6,7], and Timothy I. Eglinton[1]

[1]Geological Institute, ETH Zurich, Zurich, Switzerland, [2]Now at Department of Earth and Planetary Sciences, Harvard University, Cambridge, MA, USA, [3]Laboratory for Marine Ecology and Environmental Science, Qingdao National Laboratory for Marine Science and Technology, Qingdao, China, [4]Key Laboratory of Marine Chemistry Theory and Technology (Ocean University of China), Ministry of Education, Qingdao, China, [5]Center for Marine Environmental Studies, Ehime University, Matsuyama, Japan, [6]Laboratory for Ion Beam Physics, Department of Physics, ETH Zurich, Zurich, Switzerland, [7]Scottish Universities Environmental Research Centre, Glasgow, UK

Abstract Understanding the effects of hydrodynamic forcing on organic matter (OM) composition is important for assessment of organic carbon (OC) burial in marginal seas on regional and global scales. Here we examine the relationships between regional oceanographic conditions (bottom shear stress), and the physical characteristics (mineral surface area and grain size) and geochemical properties (OC content [OC%] and carbon isotope compositions [^{13}C, ^{14}C]) of a large suite of surface sediments from the Chinese marginal seas to assess the influence of hydrodynamic processes on the fate of OM on shallow continental shelves. Our results suggest that ^{14}C content is primarily controlled by organo-mineral interactions and hydrodynamically driven resuspension processes, highlighted by (i) positive correlations between ^{14}C content and OC% (and surface area) and (ii) negative correlations between ^{14}C content and grain size (and bottom shear stress). Hydrodynamic processes influence ^{14}C content due to both OC aging during lateral transport and accompanying selective degradation of OM associated with sediment (re) mobilization, these effects being superimposed on the original ^{14}C characteristics of carbon source. Our observations support the hypotheses of Blair and Aller (2012, https://doi.org/10.1146/annurev-marine-120709-142717) and Leithold et al. (2016, https://doi.org/10.1016/j.earscirev.2015.10.011) that hydrodynamically driven sediment translocation results in greater OC ^{14}C depletion in broad, shallow marginal seas common to passive margin settings than on active margins. On a global scale, this may influence the extent to which continental margins act as net carbon sources and sinks. Our findings thus suggest that hydrodynamic processes are important in shaping the nature, dynamics, and magnitude of OC export and burial in passive marginal seas.

1. Introduction

Understanding the fate of organic matter (OM) deposited in continental margin sediments is critical for constraining carbon cycle models, including carbon exchange between terrestrial, oceanic, and atmospheric carbon reservoirs (Bauer et al., 2013; Bianchi et al., 2018; Bianchi & Allison, 2009; Hedges & Keil, 1995). Large amounts of marine and terrestrial organic carbon (OC) are produced in and delivered to river-dominated marginal seas (Bianchi et al., 2018; Blair & Aller, 2012; Hedges & Keil, 1995). Preservation of OM in continental margin sediments is mainly attributed to physical protection via association with minerals (Arnarson & Keil, 2007; Burdige, 2005, 2007; Mayer, 1994). Marginal sea systems are highly dynamic and heterogeneous, with spatially diverse sediment transport processes as well as OC inputs that influence the distribution and composition of sedimentary OM (Bao et al., 2016; Bianchi et al., 2018). Significant gaps remain in our understanding of relationships between transport processes and OM characteristics; spatially comprehensive investigations are needed to deconvolve the intertwined influences of carbon sources and transport processes on the composition and distribution of OM accumulating in continental shelf sediments (e.g., van der Voort et al., 2018).

Surface sediments of river-dominated margins typically exhibit significant variability in OC radiocarbon ($^{14}C_{OC}$) content (Bao et al., 2016; Bianchi et al., 2016; Canuel & Hardison, 2016; Griffith et al., 2010; Wakeham & McNichol, 2014). While this variability can be partly attributed to variations in OC sources,

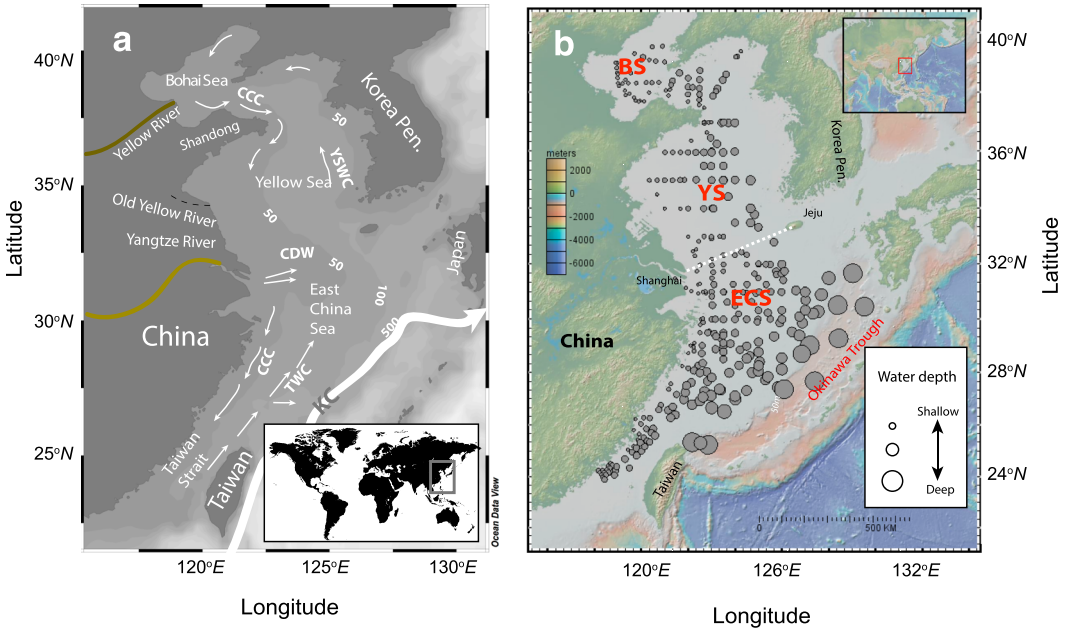

Figure 1. (a) The Chinese Marginal Sea (CMS) study area. The white arrows indicate prevailing current directions (modified from Chen, 2009): the Chinese Coastal Current (CCC), the Yellow Sea Warm Current (YWC), the Kuroshio Current (KC), Yangtze (Changjiang) Diluted Water (CDW), and the Taiwan Warm Current (TWC). (b) Subregions of the CMS (delineated by the white dashed line): The Yellow Sea-Bohai Sea (BS-YS) and the East China Sea (ECS) as defined by (Harris et al., 2014; Saito et al., 1998; Lie & Cho, 2016). Bubble sizes represent the approximate water depth at each sample location (larger size meaning greater water depth; minimum and maximum bubble sizes corresponding to approximately 20 and 1,000 m, respectively).

there is evidence that hydrodynamic processes also influence $^{14}C_{OC}$ content of marine sediments (Bao et al., 2016, 2018; Bröder et al., 2018; Cathalot et al., 2013; Inthorn et al., 2006; Keil et al., 2004; Kusch, Eglinton, et al., 2010; Kusch, Kashiyama, et al., 2010; Ohkouchi et al., 2002; Pedrosa-Pàmies et al., 2013; Mollenhauer & Eglinton, 2007; Mollenhauer et al., 2003, 2005, 2006, 2007, 2008; Shah et al., 2008; Tesi et al., 2008, 2010, 2014, 2016; Table S1). In addition to inducing widespread dispersal of sediments, hydrodynamic processes also affect the extent of degradation and compositional characteristics of associated OM (Bao et al., 2016, 2018; Bröder et al., 2018; Pedrosa-Pàmies et al., 2013; Thomsen & Gust, 2000). For instance, the *sortable silt* component of sediment that is most prone to resuspension and redistribution exhibits relatively low OC loadings (Bao et al., 2016), likely due to enhanced degradation and preferential removal of labile OC during entrainment in deposition-resuspension loops (Aller & Blair, 2004, 2006; Bröder et al., 2018; Keil et al., 2004). These processes are considered to alter both stable carbon ($^{13}C_{OC}$) and $^{14}C_{OC}$ compositions of residual OM (Bao et al., 2016). However, incomplete knowledge of the interplay between hydrodynamic processes, OM-mineral associations, selective protection, and attenuation or modification of OM during sediment translocation presently limits our understanding of carbon cycling on continental shelves.

In this study, we have undertaken an extensive survey of mineral-specific surface area (SA), mean grain size, and the OC content (OC%) and $^{13}C_{OC}$, $^{14}C_{OC}$ in surface sediments from an large passive marginal sea system: the Chinese marginal seas (abbreviation: CMS), encompassing the Bohai Sea (BS), the Yellow Sea (YS), and the East China Sea (ECS; Figure 1). Spatial variations in these sedimentological and geochemical properties are examined within a hydrodynamic context (bottom shear stress). Broader, global-scale implications are discussed in the context of carbon cycling on passive and active continental margins.

2. Sampling and Methods

2.1. Study Area and Sampling

The CMS, as a passive marginal sea system, constitutes the interface between the Eurasian continent and Pacific Ocean. The CMS receives vast quantities of terrestrial material primarily from the Yellow River (Huang He) and Yangtze (Changjiang) River that originate in the highlands of the Tibetan Plateau and integrate materials emanating from their extensive drainage basins. The Yellow River alone exports ~150 Mt/

year sediment to the BS (Wang et al., 2010, 2011). While the coastal area adjacent to the Yellow River delta acts as a sediment sink in summer, these sediments are subject to subsequent remobilization triggered by winter storms (Yang et al., 2011) and are exported to the YS through the seasonal currents (e.g., Chinese Coastal Current [CCC]; Yang & Liu, 2007; Figure 1a). About 30% of the Yellow River sediment is estimated to reach the central YS (Liu et al., 2004; Yang & Liu, 2007). The Yangtze River discharges ~110 Mt/year sediment into the ECS (Yang et al., 2014, 2015). Although a large fraction of Yangtze-derived sediments is deposited proximal to the river mouth, significant amounts of material are dispersed by seasonal shelf currents (Gao & Collins, 2014). In winter, Yangtze-derived, fine-grained sediments are carried southward by an intensified CCC that transports materials parallel to the coastline. Due to these prevailing southward flowing coastal currents, an elongated distal subaqueous mud wedge overwhelmingly derived from Yangtze River materials has developed on the inner shelf of the ECS. In spring, Changjiang Diluted Water strengthens and turns eastward, while the CCC in the ECS weakens and the Taiwan Warm Current begins to intensify. In summer, Taiwan-derived sediments are delivered westward, while the Changjiang Diluted Water transports fluvially derived sediment eastward across the ECS (Figure 1a). In fall, the Yellow Sea Warm Current that originates from the Kuroshio Current dominates the circulation from the ECS to the YS.

These seasonal currents play a crucial role in the mobilization, transport, and dispersal of fluvially derived sediments and associated OM of both terrestrial and marine origin (Liu et al., 2007; Yang & Liu, 2007; Yao et al., 2014, 2015), with broader-scale hydrodynamic processes likely driven by interactions between both local and regional current systems (Chen, 2009; Figure 1a). These spatially and temporally complex hydrodynamic conditions can lead to widespread dispersal of suspended sediment and associated OM in the CMS. In order to develop regional-scale assessments of OC fate influenced by hydrodynamic processes and keep a uniform regional delineation for comparative analysis with prior studies, we separate the CMS into the BS-YS and ECS, delineated by a line between Shanghai and Jeju Island (Figure 1b), according to prior studies of Saito et al. (1998), Harris et al. (2014), and Lie and Cho (2016).

Surface sediment (0–2 cm) samples (n = 270) were collected in 2011, 2013 on the R/V *Dongfanghong II*, and in 2014 on the R/V *Yanping II*. The samples were retrieved by box-corer or grab sampler and stored at −20 °C prior to analysis. Combined with published results, the database including oceanographic conditions, physical characteristics, geochemical properties, and carbon isotope compositions of surface sediment samples in the CMS is shown in Figure 2 and Table S2 (n = 358).

2.2. Mineral-Specific Surface Area Analysis

After freeze-drying, aliquots of a subset of sediment samples (n = 183) were heated at 350 °C for 24 hr in order to remove OM (Mayer, 1994), outgassed at 350 °C under vacuum for 2 hr to ensure complete removal of moisture, and then measured using a 5-point Brunauer-Emmett-Teller (BET) method on a NOVA 4000 (Quantachrome Instruments) in order to determine mineral-specific SA (Keil et al., 1997; Mayer, 1994; Tao et al., 2015). Based on replicate measurements (n = 4) of one standard sample, we estimate a standard error of ± ~2–3%.

2.3. Bulk Organic Carbon Isotopic Analysis

Aliquots of freeze-dried bulk sediment samples (n = 270) were analyzed for stable carbon isotope composition of bulk OM ($\delta^{13}C_{OC}$) on a Vario MICRO cube elemental analyzer (Elementar Analysensysteme GmbH) coupled to a VisION stable isotope mass spectrometer (Isoprime Ltd, UK) that was calibrated against standard materials (Laboratory of Ion Bean Physics, ETH Zurich). Prior to analysis, inorganic carbon was removed by fumigation in the presence of HCl (37%, 72 hr) and drying over NaOH pellets (72 hr) in a desiccator at 60 °C (Bao et al., 2016; Tao et al., 2015). Resulting $\delta^{13}C_{OC}$ values were measured to a precision of less than 0.1‰, based on standards.

Methods and results from ^{14}C analysis of bulk OC in sediment samples have been reported previously (n = 358; Bao et al., 2016). Sampling dates are shown in Table S2.

2.4. Bottom Shear Stress

Resuspension phenomena are pervasive in shallow marginal seas under conditions when bottom shear stress exceeds critical threshold for initiation of surface sediment motion (McCave, 1986; McCave & Hall, 2006). In this context, the magnitude of bottom shear stress is an important consideration in sediment mobilization

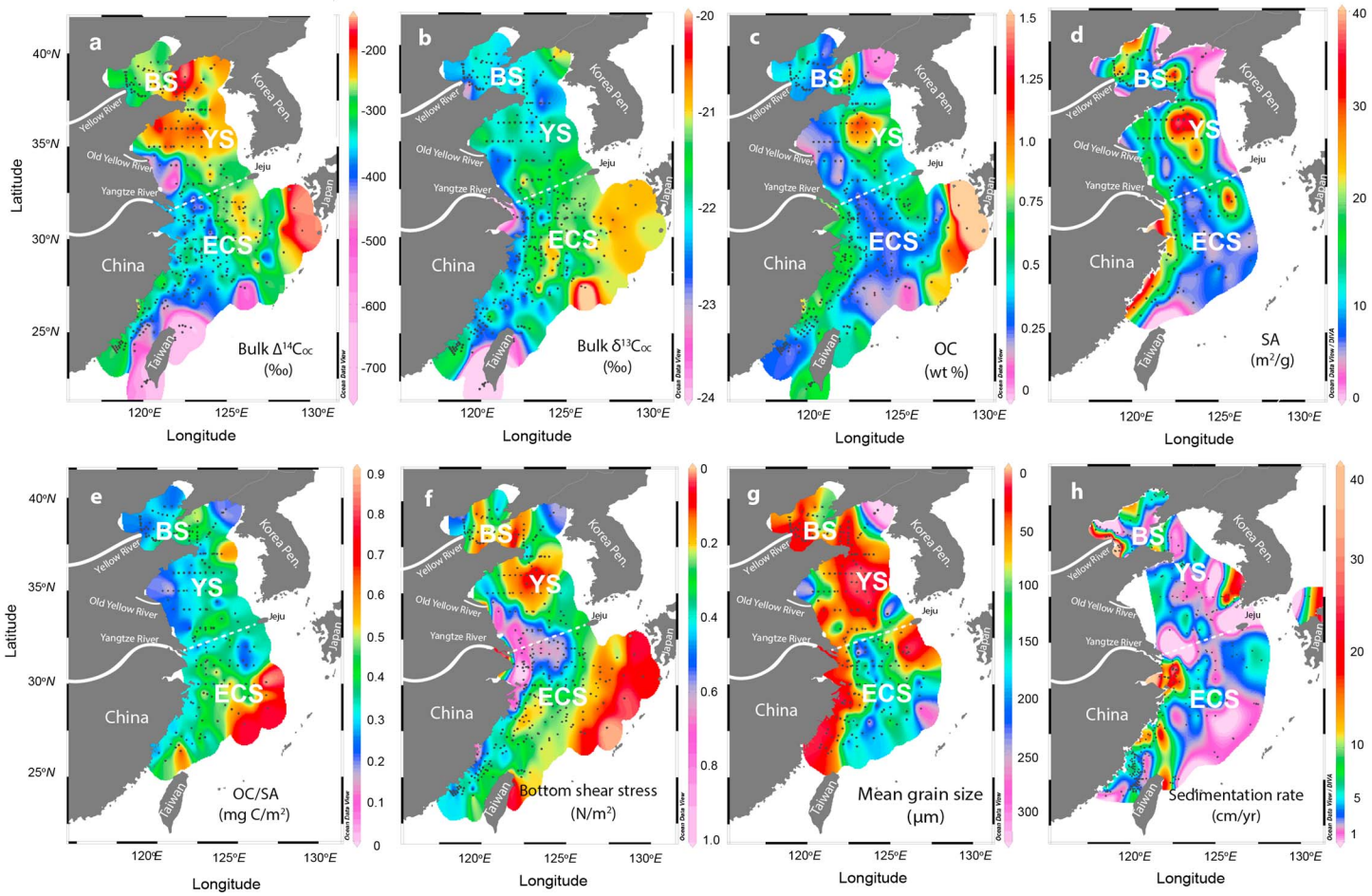

Figure 2. Spatial variability in (a) radiocarbon content of bulk OM ($\Delta^{14}C_{OC}$; Bao et al., 2016), (b) stable carbon isotope composition of bulk OM ($\delta^{13}C_{OC}$), (c) bulk OC content (OC%; Bao et al., 2016), (d) mineral-specific surface area (SA; m^2/g), (e) organic carbon loading (OC:SA, mg C/m^2), (f) bottom shear stress (N/m^2), (g) mean grain size (μm; Bao et al., 2016), and (h) sedimentation rate (Qiao et al., 2017, reference therein).

and dispersal. Spatial variability in shear stress in the CMS is poorly constrained and certainly varies temporally. Nonetheless, some insights can be gleaned from tidal currents.

Based on established relationships between bottom current velocity (shear stress), sediment grain size, and sediment resuspension (McCave, 1986; Thomsen & Gust, 2000), there is ample potential for sediment mobilization and dispersal over this large continental shelf system (Milliman et al., 1985). To understand these potential influences on observed spatial variations in surface sediment properties, we calculated the bottom stress ($\overrightarrow{\tau_b}$) at our sampling sites using a hydrodynamic model (Wang et al., 2008) as follows:

$$\tau_b^x = \rho C_d u \sqrt{u^2 + v^2} \quad (1)$$

$$\tau_b^y = \rho C_d v \sqrt{u^2 + v^2} \quad (2)$$

where τ_b^x and τ_b^y are the eastward and northward components of bottom shear stress, u and v are the eastward and northward component of bottom currents, ρ is water density, and C_d is the bottom drag coefficient. The bottom current is composed of tidal components and a subtidal component, in which the tidal currents are a superposition of several tidal constituents (M_2, S_2, K_1, and O_1) with each tidal constituent having a fixed period. In the BS, YS, and ECS (<200-m water depth), the amplitude of the M_2 tidal current (principal lunar semidiurnal and the strongest tidal constituent) is over 0.5 m/s (Guo & Yanagi, 1998), whereas

Table 1
Significant Spearman Correlations Between $\Delta^{14}C$ and Various Parameters in the CMS

Parameters	$\Delta^{14}C$ (‰)
Water depth (m)	-
SA (m^2/g)	0.29 ($p < 0.0005$)
TOC (%)	0.32 ($p < 0.0005$)
OC/SA (C mg/m^2)	-
$\delta^{13}C$ (‰)	-
Mean grain size (μm)	−0.19 ($p < 0.05$)
Bottom shear stress (N/m^2)	−0.46 ($p < 0.0005$)

Note: Hyphen indicates nonsignificant correlation.

subtidal currents have a magnitude of 0.2 m/s or less (Lie & Cho, 2016). We thus argue that the former is the major contributor to bottom shear stress. A harmonic analysis program (T-tide; Pawlowicz et al., 2002) is then used to obtain the amplitude and phase of tidal current and bottom shear stress with the periods encompassing all tidal constituents at each of the grid points in our hydrodynamic model. We use a grid size of 1/18 degree in meridional and zonal directions and 20 layers in the vertical direction (Wang et al., 2008). Among tidal constituents used in the model (Wang et al., 2008), M_2 tidal current is the strongest with a magnitude at least twice that of other tidal constituents (Guo & Yanagi, 1998; Lie & Cho, 2016). Consequently, the bottom shear stress associated with M_2 tidal period is at least 4 times stronger than that related to other tidal constituent periods because the bottom shear stress is proportion to square of bottom current (equations (1) and (2)). As an approximation, we therefore use the amplitude of bottom shear stress with M_2 tidal period to represent the amplitude of bottom shear stress in the CMS (Figure 2f). Wave-induced bottom shear stress is over one magnitude smaller than the tide-induced bottom shear stress (Luo et al., 2017) and is therefore not considered.

2.5. Statistical Analysis

In order to evaluate and quantify the significance of correlations between various key parameters related to hydrodynamic processes (e.g., water depth and bottom shear stress) and geochemical characteristics (e.g., OC% $\Delta^{14}C_{OC}$), Spearman correlations were determined (significant for $p < 0.05$) for the subset of CMS samples ($n = 194$), which was determined for all parameters (Table 1). The latter method was chosen to account for nonparametric nature of the data. The statistical analyses were applied using the open-source statistical software, "R," version 3.2.3.

3. Results and Discussion

3.1. OC Characteristics of Surface Sediments in the BS-YS and ECS

Spatial variations in $\Delta^{14}C_{OC}$ for bulk sediments from the CMS were previously described by Bao et al. (2016). The measured $\Delta^{14}C_{OC}$ values exhibit a general decrease with decreasing OC% (Figure 3). The lower $\Delta^{14}C_{OC}$ values in BS-YS samples may be due to prolonged resuspension and reworking of sediments on the inner shelf (Bao et al., 2016, 2018), as well as inputs of preaged OC from the Yellow River (Tao et al., 2015; Wang et al., 2012). While some lower-OC% and ^{14}C-depleted samples from the ECS are from shallow regions, a substantial proportion (≳35%) of samples with the low $\Delta^{14}C_{OC}$ values (i.e., $\Delta^{14}C_{OC}$ less than ~ −400‰) originate from deeper regions (Figure 3). The latter observation might be explained by export and supply of preaged OM from small rivers draining the Taiwan Island (Hilton et al., 2011; Kao et al., 2014), while the lower $\Delta^{14}C_{OC}$ values from shallower, inner-shelf regions may reflect the supply of ^{14}C-depleted OM from the Yangtze River and subsequent sediment remobilization processes (Bao et al., 2016; Li et al., 2012; Wu et al., 2013). Provenance analyses based on clay mineralogy indicate that the Yangtze River is the predominant source for fine-grained sediments in shallower regions of the ECS (Qiao et al., 2017; Xu et al., 2009), and it is therefore unlikely that preaged OM from Taiwanese rivers is the primary driver of the depleted $^{14}C_{OC}$ in shallow ECS regions. Furthermore, van der Voort et al. (2018) found that Taiwan acts as a point source with a primarily local impact. In addition, sedimentation rates along the coast of the ECS are high (>5 cm/year; Figure 2h), and given this as well as sediment mixed layer depths on the order of ~10 cm (based on ^{210}Pb analysis; Su & Huh, 2002; Liu et al., 2006)—which are significantly greater than that of the sampling interval (0–2 cm)—upward mixing of older OC due to

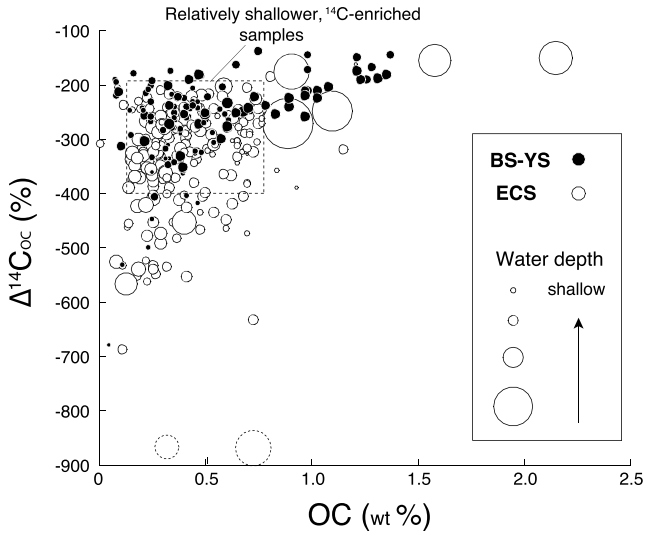

Figure 3. Relationship between $\Delta^{14}C$ values and OC% in the CMS surface sediments. Bubble sizes correspond to approximate water depth (ranging between approximately 20 and 1,000 m for smallest and largest symbols). The two dashed circles in the right panel correspond to marine sediments surround Taiwan Island.

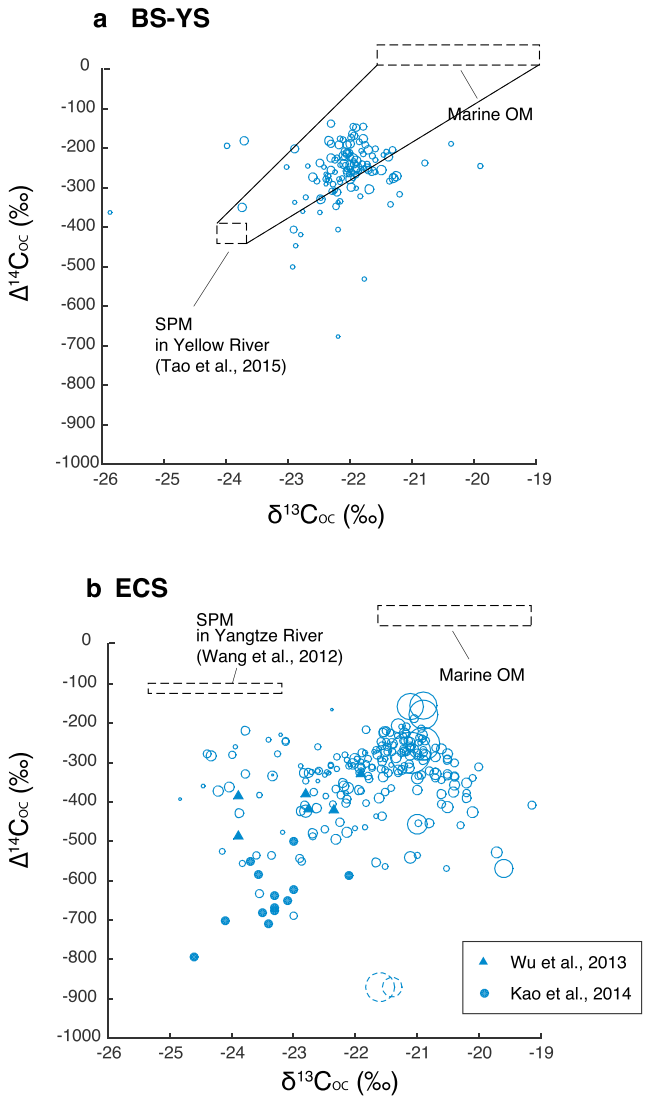

Figure 4. Bulk $\Delta^{14}C_{OC}$ versus $\delta^{13}C_{OC}$ values of samples from the (a) Bohai Sea-Yellow Sea (BS-YS) and (b) East China Sea (ECS). Bubble sizes correspond to approximate water depth. The dashed boxes indicate approximate ranges of $\Delta^{14}C_{OC}$ and $\delta^{13}C_{OC}$ values of marine OM (Blair & Aller, 2012; Wang et al., 2016) and of Yellow and Yangtze River suspended particle organic matter (SPM; Marwick et al., 2015; Tao et al., 2015; Wang et al., 2012). The data from Wu et al. (2013) and Kao et al. (2014) (solid symbols) are plotted without water depth information in the lower panel.

bioturbation is unlikely to account for the low $\Delta^{14}C_{OC}$ values observed. We also note that many low-OC% samples exhibit a range of $\Delta^{14}C_{OC}$ values (Figure 3, dashed square). Therefore, while the $\Delta^{14}C_{OC}$ of sedimentary OM in the CMS exhibits significant positive correlation with OC% (0.32, $p < 0.0005$; Table 1), our findings suggest that a complex suite of processes underpins this relationship and hence influences the fate of OC in this shallow marginal sea system.

The $\delta^{13}C_{OC}$ values of surface sediments in the CMS exhibit large spatial variability, ranging from −25.9 to −19.1‰ (Figure 2b; n = 358). In general, depleted $\delta^{13}C_{OC}$ values are found in the prodelta regions, along the coast (inner shelf) of the CMS, Northern YS, and adjacent to Taiwan, whereas relatively high $\delta^{13}C_{OC}$ values are evident on the outer-shelf and slope of the ECS extending to the Okinawa Trough (Figure 2b). These $\delta^{13}C_{OC}$ values reflect contributions from different sources of sedimentary OC (Blair & Aller, 2012), with the observed spatial pattern of $\delta^{13}C_{OC}$ values suggesting that point sources (i.e., OC discharge from rivers) may have regional impacts. In the BS-YS, $\delta^{13}C_{OC}$ values generally fall within a narrower range, from ~ −23 to −21‰ (ave. −22.1 ± 0.6‰, n = 137), lying between values for corresponding marine and fluvial (Yellow River) end-members (Figure 4a). Despite the likely influence of aging and/or selective degradation of OM in the BS-YS during sediment redistribution (Bao et al., 2016, 2018; Tao et al., 2016), these processes do not clearly manifest themselves in a $\Delta^{14}C_{OC}$-$\delta^{13}C_{OC}$ scatter plot (Figure 4a). This may be due to the replacement of terrestrial OM by ^{13}C-enriched (Keil et al., 1997) and younger (higher $\Delta^{14}C_{OC}$ values) marine OM (Blair & Aller, 2012).

In contrast to the BS-YS system, $\Delta^{14}C_{OC}$-$\delta^{13}C_{OC}$ values of ECS sediments fall outside of a simple mixing between two end-members of marine and terrestrial OM (Figure 4b). In this regime, the Yangtze River is the dominant sediment source (Qiao et al., 2017), with mean annual sediment discharge for the other smaller rivers contributing <25% (~1.0×10^5 Mt) of that of the Yangtze (Qiao et al., 2017). Based on the studies of Wang et al. (2012), the $\Delta^{14}C_{OC}$ values of suspended particulate matter (SPM) in the Yangtze River are relatively high (~ −110‰) compared to those of the Yellow River. Moreover, ECS surface sediments exhibits a larger variation of ^{14}C contents compared with the BS-YS (Figure 4). Again, while Taiwanese rivers may supply preaged OC to the ECS, the sediment load from western Taiwan is much smaller (<16%) than that of the Yangtze River (Qiao et al., 2017). Additionally, the bulk sediment emanating from Taiwan fluvial systems empties into the Taiwan Strait or southern and eastern trough areas (Kao et al., 2014; Liu et al., 2013; Xu et al., 2009) and is therefore unlikely to contribute significantly to the variability in $\Delta^{14}C_{OC}$ values of surface sediments across the entire ECS (Figure 4b).

Recently, Bao et al. (2016, 2018) provided evidence for OM aging during the lateral sediment redistribution in the CMS. Both ^{14}C decay associated with protracted entrainment in repeated resuspension-deposition loops on the shallow inner shelf (Zhu et al., 2006) and removal of labile (i.e., ^{14}C- and ^{13}C-enriched) OM could result in lower $\Delta^{14}C_{OC}$ ($\delta^{13}C_{OC}$) values (Bao et al., 2016; Mollenhauer & Eglinton, 2007). Samples with lower $\delta^{13}C$ values in Figure 2b (blue regions in the ECS) are also primarily sediments from the inner shelf, suggesting that this region is characterized by enhanced terrestrial OC contributions and/or selective degradation of ^{13}C-enriched OC. Additionally, sediments underlying deeper waters (e.g., >100 m) are relatively enriched in $^{14}C_{OC}$ and $^{13}C_{OC}$ (Figures 2b and 4b), implying that ^{14}C aging and selective degradation processes are most pronounced on the inner shelf relative to deeper regions.

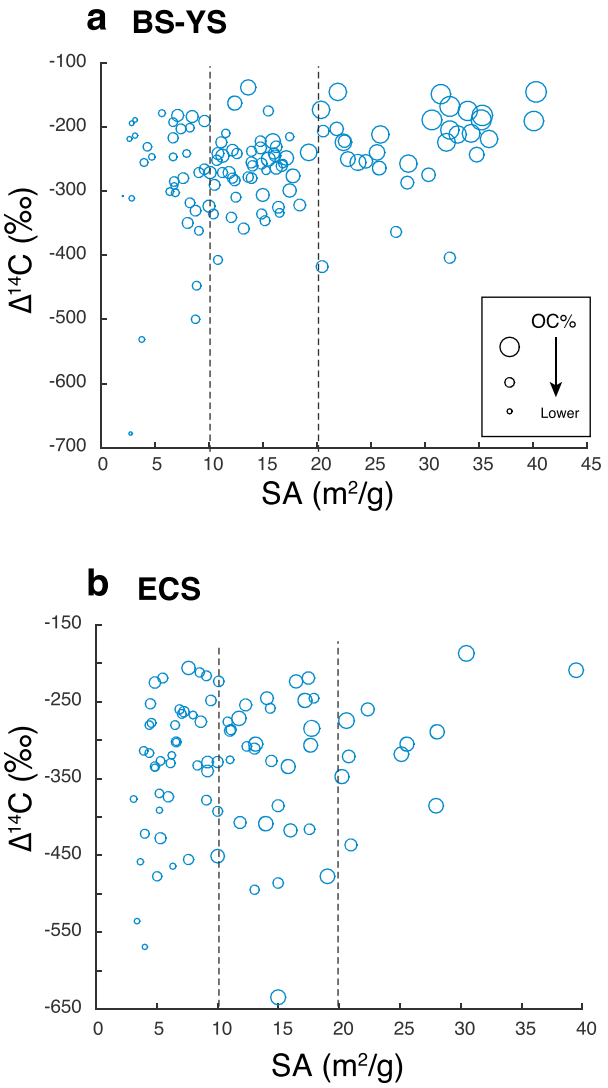

Figure 5. Relationship between $\Delta^{14}C_{OC}$ values and SA in the (a) Bohai Sea-Yellow Sea (BS-YS) and (b) East China Sea (ECS). The bubble size represents the OC% (ranging between approximately 0.1 and 1.5% for smallest and largest symbols).

3.2. Influence of Hydrodynamic Processes on Fate of OC

Grain size influences both hydrodynamic properties and SA of marine sediments (Mayer, 1994; McCave & Hall, 2006). Effects of hydrodynamic processes on OC% and carbon isotope composition are closely intertwined due to physical protection through OM association with mineral surfaces (positive Spearman correlation [0.29] of $\Delta^{14}C_{OC}$ with SA, $p < 0.0005$; Table 1), thereby complicating assessment of the influence of hydrodynamic processes on $^{14}C_{OC}$-$^{13}C_{OC}$ characteristics. Hydrodynamic processes should manifest themselves through differential (re) mobilization and dispersal of sediment grain sizes (McCave, 1986; Thomsen & Gust, 2000; Thomsen & McCave, 2000), which, in turn will influence the $\Delta^{14}C_{OC}$ values of associated OM. For instance, Bao et al. (2016) suggested that older OC in the sortable silt fraction (20–63 μm) of inner shelf sediments reflects the susceptibility of this fraction to cyclic resuspension, transport, and deposition within the benthic nepheloid layer.

In the CMS, grain size is negatively correlated with SA (Figure S1), with the latter invoked as a control on OM preservation in continental margin sediments (Blair & Aller, 2012; Mayer, 1994). The sortable silt fractions (20–63 μm) and coarser sediments (>63 μm) correspond to SA values with a range of 10–20 m^2/g and < 10 m^2/g, respectively. Although high SA sediments can be expected to have generally higher OC% as compared to lower SA sediments, and sediment characterized by higher OC% also exhibit higher $\Delta^{14}C_{OC}$ values (Figure 3), we note that there is no significant difference in $\Delta^{14}C_{OC}$ values among the three corresponding SA ranges (>20, 10–20, and <10 m^2/g, respectively; Figures 5 and S2). This suggests that mineral surface protection of fresher OM associated with sortable silt fractions (i.e., SA 10–20 m^2/g) may be undermined by hydrodynamic processes. Consequently, although OC% exhibits a general correlation with $\Delta^{14}C_{OC}$ values (Figure 3), hydrodynamic processes independently exert an influence on surface sediment $\Delta^{14}C_{OC}$ values in the CMS.

General relationships between abundance of terrestrial and marine OC with respect to mineral-specific surface area (OC:SA) have emerged from studies of continental shelf sediments (Blair et al., 2003; Blair & Aller, 2012; Burdige, 2005; Coppola et al., 2007; Goñi et al., 2005; Wang et al., 2015; Wu et al., 2013). Typical OC:SA ratios for river-dominated continental shelf sediments range from 0.5 to 1.0 mg C/m^2 (Bianchi et al., 2018; Blair & Aller, 2012; Eglinton & Repeta, 2003; Hedges & Keil, 1995; Mayer, 1994). This ratio has been used as an index to assess terrestrial OM loading on sedimentary particles (Burdige, 2005; Keil et al., 1997; Wu et al., 2013) and to place constraints on terrestrial OC burial efficiency in marginal sea sediments (Burdige, 2005; Keil et al., 1997; Nuwer & Keil, 2005). In the CMS, surface sediment OC:SA ratios exhibit distinctly spatial variability (Figure 2d), with generally lower ratios in the BS-YS than in the ECS (significant difference, *t* test; Figure S3). Furthermore, while BS-YS sediments exhibit large variability in OC:SA ratios (<0.05 to >0.55 mg C/m^2; ave. 0.32 mg C/m^2, $n = 117$), they are generally higher than those of Yellow River SPM (0.18 mg OC/m^2, mean grain size: 8–17 μm; Tao et al., 2015). Interestingly, $\delta^{13}C_{OC}$ values of BS-YS sediments are relatively uniform (ave. −22.1 ± 0.6‰, $n = 123$; mean grain size: 59 μm, $n = 119$; Figure 6a), despite significant variability in $\Delta^{14}C_{OC}$ values (Figure 6b). Some samples with lower OC:SA ratios, particularly those originating from the shallower parts of the BS-YS, exhibit more scattered and generally lower $\Delta^{14}C_{OC}$ values (dashed circle, Figure 6b). These differing relationships between OC/SA ratios and $\Delta^{14}C_{OC}$ and $\delta^{13}C_{OC}$ values suggest that hydrodynamic processes influence OC isotopic composition, especially for sediments from shallower inner-shelf settings.

It has been previously observed that marine sediments accumulating proximal to the Fly (Papua New Guinea) and Columbia (northwest USA) rivers exhibited lower OC/SA ratios and higher $\delta^{13}C_{OC}$ values than those of

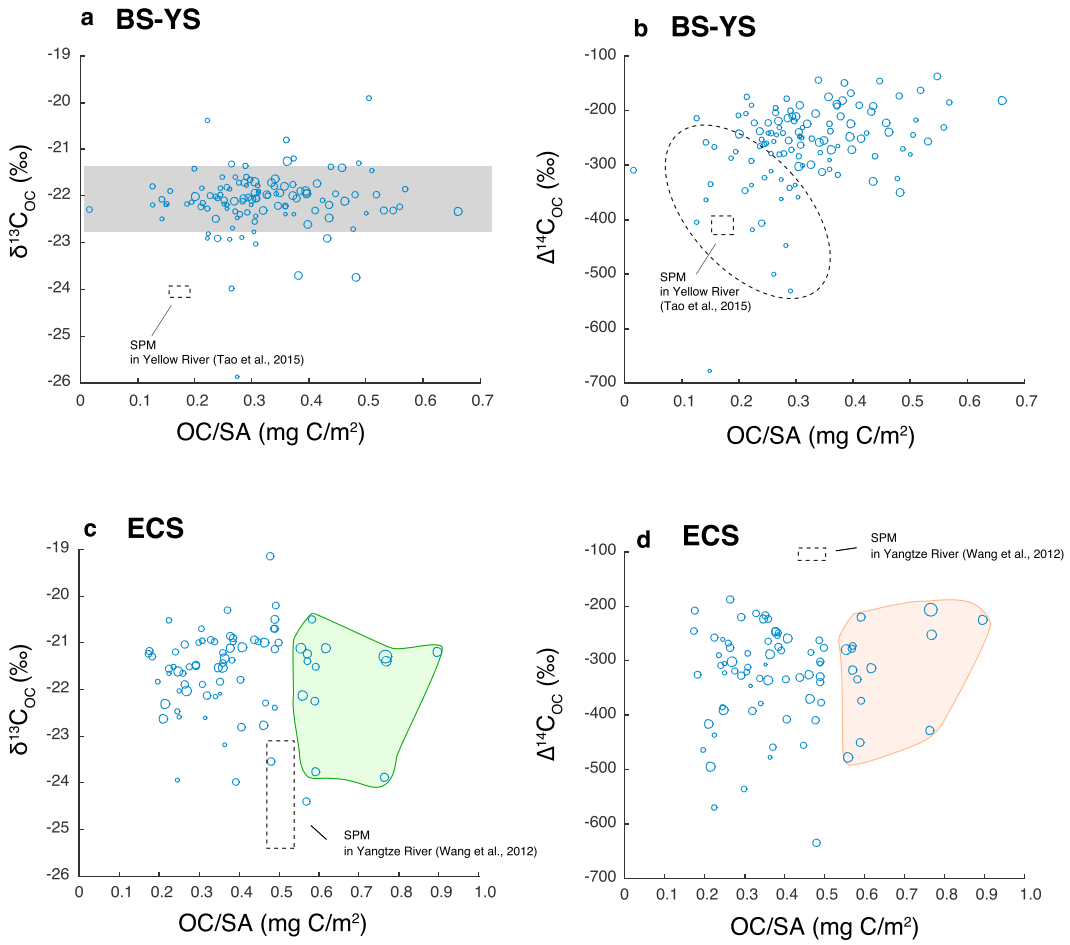

Figure 6. Relationships between carbon isotopic characteristics ($\Delta^{14}C_{OC}$, $\delta^{13}C_{OC}$) and OC:SA in surface sediments of the (a and b) Bohai Sea-Yellow Sea (BS-YS) and the (c and d) East China Sea (ECS). The bubble size represents the sample water depth; (a) the shaded area highlights the low variability in $\delta^{13}C_{OC}$ values (ave. −22.1 ± 0.6‰); (b) the dashed circle indicates the samples from shallow (<25 m) locations that are characterized by lower OC% and $\Delta^{14}C_{OC}$ values; (c and d) the green envelope shows the samples with larger OC:SA ratios and higher $\delta^{13}C_{OC}$ than SPM, and the orange envelope shows the samples with larger OC:SA ratios and lower $\Delta^{14}C_{OC}$ than SPM. The box circle indicates approximate corresponding values for SPM from the Yellow River (a and b) and Yangtze River (c and d).

corresponding riverine SPM (Keil et al., 1997). This change in OC loading has been attributed to a process of loss of terrestrial OM and replacement with marine OM on mineral surfaces. In the case of the ECS, we note that some sediments from deeper regions exhibit OC:SA ratios and $\delta^{13}C_{OC}$ values that are both higher than riverine SPM (Figure 6c, green area), whereas $\Delta^{14}C_{OC}$ values are lower than those of Yangtze River SPM (Figure 6d, orange area). This may reflect the influence of other hydrodynamic processes, such as preferential displacement of certain grain size fractions, on OM composition. Therefore, loss-and-replacement processes are unlikely to be the only cause of the observed changes of $\delta^{13}C_{OC}$ and $\Delta^{14}C_{OC}$ with OC:SA ratios.

While hydrodynamic processes are a driving factor promoting sediment resuspension (McCave, 1986; McCave et al., 1995) and contributing to the above geochemical characteristics, they are difficult to constrain from direct field observations. We therefore use bottom shear stresses calculated from a hydrodynamic model that is based on tidal forcing and circulation patterns in the CMS in order to examine the dependence of surface sediment $\Delta^{14}C_{OC}$ on hydrodynamic conditions. Our results reveal a significant negative correlation between $\Delta^{14}C_{OC}$ and bottom shear stress for the entire CMS (Spearman correlation −0.46, $p < 0.0005$; Table 1); that is, greater bottom shear stress corresponds to lower $\Delta^{14}C_{OC}$ values (^{14}C aging; Figure 2f), presumably as a consequence of processes associated with enhanced sediment mobilization

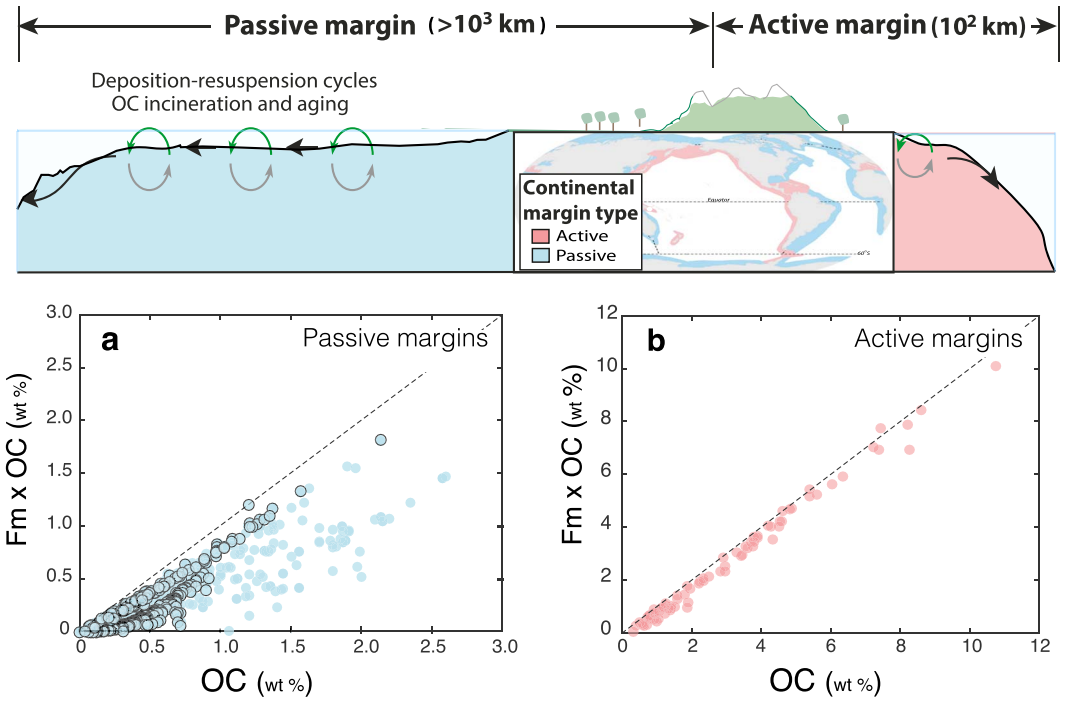

Figure 7. Fm × OC% versus OC% relationships for surface sediments from (a) passive margins and (b) active margins (supporting information; the samples from this study are highlighted by black circles). The schematic highlights the contrasting characteristics of active and passive margins (modified from Blair and Aller, 2012). In previous studies, straight-line relationships between Fm × OC% (Blair et al., 2003; Cui et al., 2017; Galy et al., 2008; Tao et al., 2015) and OC% were observed. Here Fm × OC% reflects both marine and terrestrial biogenic OM (assuming a binary mixture of end-members: ^{14}C-free ancient carbon and modern carbon with the ^{14}C content of the modern atmosphere).

and hydrodynamically induced particle sorting. Once the shear stress exceeds the critical erosion threshold, this will lead to resuspension and an abrupt increase in the concentrations of SPM in the water column. Entrainment in repeated suspension-deposition loops results in enhanced OC remineralization (Aller & Blair, 2006), with selective degradation of younger OC and hence an apparent increase in ^{14}C age (decrease in ^{14}C content) of residual OM. The OM associated with those sediments subjected to greater bottom shear stress is thus likely to exhibit lower ^{14}C contents (older OC ages). These findings suggest that hydrodynamic processes are a key factor in dictating ^{14}C content (age) of underlying sediments in the CMS.

3.3. Contrasting OC Fates on Passive and Active Margins

Sediment resuspension and redistribution is widespread on and beyond, continental margins (Hwang et al., 2010). The underlying hydrodynamic processes influence OC characteristics, likely through a combination particle sorting effects and OM-mineral surface interactions, of which ^{14}C content is perhaps most diagnostic (Table S1). Such processes may exert greater influence on passive margins that host expansive shallow continental shelf seas (e.g., BS-YS and ECS), leading to longer sediment residence and transport times (aging) and protracted entrainment in resuspension-deposition loops (Bao et al., 2018; Blair & Aller, 2012; Bröder et al., 2018). Examination of OC versus SA relationships in shelf and upper slope sediments from passive margins suggests that these systems are generally characterized by lower OC loadings (i.e., OC:SA $<$0.5 mg C/m^2) than those from active margins (OC:SA $>$1.0 mg C/m^2; Figure S4). Thus, on a global scale, OC may experience contrasting fates on active and passive margins, underlining a need to better understand relationships between physical dynamics and nature and efficiency of OC burial (Blair & Aller, 2012). While data coverage remains sparse, and additional factors (e.g., bottom oxygen concentration) are also likely important (Bianchi et al., 2018), we suggest that the distinctive physical dynamics of active and passive margins strongly influences the fate of OC.

A plot of ^{14}C content (expressed as Fraction modern [Fm]; Stuiver & Polach, 1977) × OC% versus OC% reveals the contrasting characteristics of surface sediments from active and passive margins (Figure 7). Those from

active margins fall close to a straight line, suggesting that OC content in these sediments strongly influences ^{14}C content, whereas passive margin sediments exhibit considerable scatter and fall below the 1:1 line. This implies that other factors, independent of OC%, control ^{14}C content. These may include selective degradation of OC, preferential export of OC from different carbon sources (Zonneveld et al., 2010), or lateral transport times. Decreasing ^{14}C contents associated with the latter phenomenon is independent on OC%, composition, and/or carbon source. Due to likely influence of each of these factors in passive margin systems, lower ^{14}C contents caused by lateral transport is likely often masked. However, in the case of the CMS, ancillary evidence points to a clear role for these processes as a cause for the observed scatter in this relationship. We therefore speculate that sediment resuspension and other hydrodynamically driven processes that impact on ^{14}C content are a hallmark of passive margin systems. Consequently, the type of plot exemplified in Figure 7 may prove useful in assessing relationships between continental margin dynamics and the fate of OC (Galy et al., 2008; Tao et al., 2015).

In addition to varying degrees of OC incineration linked to margin type and length scales for sediment resuspension (Figure 7; Bao et al., 2018; Blair et al., 2003; Blair & Aller, 2012; Bröder et al., 2018), the different geometries of active and passive margins have implications for dynamics and nature of OC delivered to, and buried in the deep ocean, both for the present and the geologic past (Blair et al., 2003, 2004; Drenzek et al., 2007; Leithold et al., 2016; Muller-Karger et al., 2005). For example, reduced accommodation space and sediment resuspension on continental shelves during intervals of lower sea level may help to explain elevated OC% of margin sediments during glacial maxima (Cartapanis et al., 2016; Hilton et al., 2015; Wagner et al., 2014). In this context, diminished OC remineralization on active margins and more direct OC transfer to deep ocean would correspond to a short-term OC sink, whereas more extensive processing on OM on passive margins acts as a OC source. This balance of OC source-to-sink processes on active versus passive margins may thus play an important role in regulating global carbon cycle.

4. Summary and Conclusions

Hydrodynamic processes are known to influence carbon cycling on continental margins, however, the underlying mechanisms and their impact on the distribution and characteristics of sedimentary OM remain elusive. Our in-depth survey of shallow CMS sediments reveals the following:

1. In addition to carbon provenance, bulk $^{14}C_{OC}$ contents are impacted by both organo-mineral interactions and hydrodynamically-driven resuspension processes, highlighted by (a) positive correlations between $\Delta^{14}C_{OC}$, and OC% and SA, and (b) negative correlations between $\Delta^{14}C_{OC}$, grain size, and bottom shear stress (Table 1).
2. Relationships between $^{14}C_{OC}$ contents, OC%, and SA reveal widespread influence of resuspension processes on the ^{14}C age and OC% in sediments from shallow, broad marginal seas (Figures 3 and 5).
3. Our sediment data set supports prior hypotheses that resuspension processes exert greater influence on OC fate on passive margins compared with active margins (Figure 7). This in turn may influence the extent to which continental margins act as net carbon sources and sinks globally, both for the present-day and the past.
4. The differing extents of OM processing on active and passive margins have implications of the characteristics and fate of OC exported to the interior ocean (Figure 7). Remobilization and redistribution of sedimentary OM on the continental margins thus emerge as an important component of the global oceanic carbon cycle and should be considered in budgets and fluxes of oceanic OC burial and export.

Acknowledgments
This study was supported by SNF "CAPSLOCK" project 200021_140850 (T. I. E.), by the National Natural Science Foundation of China (grants 41520104009 and 41521064, M. Z.) and by the "111" project (B13030). We acknowledge Shuqing Qiao (First Institute of Oceanography, State Oceanic Administration, Qingdao, China) and Qingqian Cui (Massachusetts Institute of Technology, USA) for assistance in collecting data. Readers can access or find the data from supporting information. There are no any conflicts of interest for any author that is apparent from our affiliations or funding.

References

Aller, R. C., & Blair, N. E. (2004). Early diagenetic remineralization of sedimentary organic C in the Gulf of Papua deltaic complex (Papua New Guinea): net loss of terrestrial C and diagenetic fractionation of C isotopes. *Geochimica et Cosmochimica Acta*, *68*, 1815–1825.

Aller, R. C., & Blair, N. E. (2006). Carbon remineralization in the Amazon-Guianas mobile mudbelt: A sedimentary incinerator. *Continental Shelf Research*, *26*, 2241–2259.

Arnarson, T. S., & Keil, R. G. (2007). Changes in organic matter–mineral interactions for marine sediments with varying oxygen exposure times. *Geochimica et Cosmochimica Acta*, *71*(14), 3545–3556.

Bao, R., McIntyre, C., Zhao, M., Zhu, C., Kao, S.-J., & Eglinton, I. T. (2016). Widespread dispersal and aging of organic carbon in the continental marginal seas. *Geology*. https://doi.org/10.1130/G37948.1

Bao, R., Uchida, M., Zhao, M., Haghipour, N., Montlucon, D., McNichol, A., et al. (2018). Organic carbon aging during across-shelf transport. *Geophysical Research Letters*, *45*. https://doi.org/10.1029/2018GL078904

Bauer, J. E., Cai, W. J., Raymond, P. A., Bianchi, T. S., Hopkinson, C. S., & Regnier, P. A. (2013). The changing carbon cycle of the coastal ocean. *Nature*, *504*, 61–70.

Bianchi, T. S., & Allison, M. A. (2009). Large-river delta-front estuaries as natural "recorders" of global environmental change. *Proceedings of the National Academy of Sciences*, *106*, 8085–8092.

Bianchi, T. S., Cui, X., Blair, N. E., Burdige, D. J., Eglinton, T. I., & Galy, V. (2018). Centers of organic carbon burial and oxidation at the land-ocean interface. *Organic Geochemistry*, *115*, 138–155.

Bianchi, T. S., Schreiner, K. M., Smith, R. W., Burdige, D. J., Woodard, S., & Conley, D. J. (2016). Redox effects on organic matter storage in coastal sediments during the Holocene: A biomarker/proxy perspective. *Annual Review of Earth and Planetary Sciences*, *44*, 295–319.

Blair, N. E., & Aller, R. C. (2012). The fate of terrestrial organic carbon in the marine environment. *Annual Review of Marine Science*, *4*, 401–423.

Blair, N. E., Leithold, E. L., & Aller, R. C. (2004). From bedrock to burial: the evolution of particulate organic carbon across coupled watershed-continental margin systems. *Marine Chemistry*, *92*(1), 141–156.

Blair, N. E., Leithold, E. L., Ford, S. T., Peeler, K. A., Holmes, J. C., & Perkey, D. W. (2003). The persistence of memory: the fate of ancient sedimentary organic carbon in a modern sedimentary system. *Geochimica et Cosmochimica Acta*, *67*, 63–73.

Bröder, L., Tesi, T., Andersson, A., Semiletov, I., & Gustafsson, Ö. (2018). Bounding cross-shelf transport time and degradation in Siberian-Arctic land-ocean carbon transfer. *Nature Communications*. https://doi.org/10.1038/s41467-018-03192-1

Burdige, D. J. (2005). Burial of terrestrial organic matter in marine sediments: A re-assessment. *Global Biogeochemical Cycles*, *19*, GB4011. https://doi.org/10.1029/2004GB002368

Burdige, D. J. (2007). Preservation of organic matter in marine sediments: Controls, mechanisms, and an imbalance in sediment organic carbon budgets? *Chemical Reviews*, *107*, 467–485.

Canuel, E. A., & Hardison, A. K. (2016). Sources, ages, and alteration of organic matter in estuaries. *Annual Review of Marine Science*, *8*, 409–434.

Cartapanis, O., Bianchi, D., Jaccard, S. L., & Galbraith, E. D. (2016). Global pulses of organic carbon burial in deep-sea sediments during glacial maxima. *Nature Communications*, *7*. https://doi.org/10.1038/ncomms10796

Cathalot, C., Rabouille, C., Tisnérat-Laborde, N., Toussaint, F., Kerhervé, P., Buscail, R., et al. (2013). The fate of river organic carbon in coastal areas: A study in the Rhône River delta using multiple isotopic ($\delta^{13}C$, $\Delta^{14}C$) and organic tracers. *Geochimica et Cosmochimica Acta*, *118*, 33–55.

Chen, C.-T. A. (2009). Chemical and physical fronts in the Bohai, Yellow and East China seas. *Journal of Marine Systems*, *78*, 394–410.

Coppola, L., Gustafsson, Ö., Andersson, P., Eglinton, T. I., Uchida, M., & Dickens, A. F. (2007). The importance of ultrafine particles as a control on the distribution of organic carbon in Washington Margin and Cascadia Basin sediments. *Chemical Geology*, *243*, 142–156.

Cui, X., Bianchi, T. S., & Savage, C. (2017). Erosion of modern terrestrial organic matter as a major component of sediments in fjords. *Geophysical Research Letters*, *44*, 1457–1465. https://doi.org/10.1002/2016GL072260

van der Voort, T. S., Mannu, U., Blattmann, T. M., Bao, R., Zhao, M., & Eglinton, T. I. (2018). Deconvolving the fate of carbon in coastal sediments. *Geophysical Research Letters*, *45*. https://doi.org/10.1029/2018GL077009

Drenzek, N. J., Montluçon, D. B., Yunker, M. B., Macdonald, R. W., & Eglinton, T. I. (2007). Constraints on the origin of sedimentary organic carbon in the Beaufort Sea from coupled molecular ^{13}C and ^{14}C measurements. *Marine Chemistry*, *103*(1), 146–162.

Eglinton, T. I., & Repeta, D. J. (2003). *Organic matter in the contemporary ocean, treatise on geochemistry*. Pergamon: Oxford press.

Galy, V., Beyssac, O., France-Lanord, C., & Eglinton, T. (2008). Recycling of graphite during Himalayan erosion: A geological stabilization of carbon in the crust. *Science*, *322*, 943–945.

Gao, S., & Collins, M. (2014). Holocene sedimentary systems on continental shelves. *Marine Geology*, *352*, 268–294.

Goñi, M. A., Yunker, M. B., Macdonald, R. W., & Eglinton, T. I. (2005). The supply and preservation of ancient and modern components of organic carbon in the Canadian Beaufort Shelf of the Arctic Ocean. *Marine Chemistry*, *93*(1), 53–73.

Griffith, D. R., Martin, W. R., & Eglinton, T. I. (2010). The radiocarbon age of organic carbon in marine surface sediments. *Geochimica et Cosmochimica Acta*, *74*(23), 6788–6800.

Guo, X., & Yanagi, T. (1998). Three dimensional structure of tidal current in the East China Sea and the Yellow Sea. *Journal of Oceanography*, *54*, 651–668.

Harris, P., Macmillan-Lawler, M., Rupp, J., & Baker, E. (2014). Geomorphology of the oceans. *Marine Geology*, *352*, 4–24.

Hedges, J. I., & Keil, R. G. (1995). Sedimentary organic matter preservation: an assessment and speculative synthesis. *Marine Chemistry*, *49*, 81–115.

Hilton, R. G., Galy, A., Hovius, N., Horng, M.-J., & Chen, H. (2011). Efficient transport of fossil organic carbon to the ocean by steep mountain rivers: An orogenic carbon sequestration mechanism. *Geology*, *39*, 71–74.

Hilton, R. G., Galy, V., Gaillardet, J., Dellinger, M., Bryant, C., O'regan, M., et al. (2015). Erosion of organic carbon in the Arctic as a geological carbon dioxide sink. *Nature*, *524*(7563), 84–87.

Hwang, J., Druffel, E. R., & Eglinton, T. I. (2010). Widespread influence of resuspended sediments on oceanic particulate organic carbon: Insights from radiocarbon and aluminum contents in sinking particles. *Global Biogeochemical Cycles*, *24*, GB4016. https://doi.org/10.1029/2010GB003802

Inthorn, M., Mohrholz, V., & Zabel, M. (2006). Nepheloid layer distribution in the Benguela upwelling area offshore Namibia. *Deep Sea Research Part I: Oceanographic Research Papers*, *53*, 1423–1438.

Kao, S. J., Hilton, R. G., Selvaraj, K., Dai, M., Zehetner, F., Huang, J.-C., et al. (2014). Preservation of terrestrial organic carbon in marine sediments offshore Taiwan: mountain building and atomospheric carbon dioxide sequestation. *Earth Surface Dynamics*, *2*, 127–139.

Keil, R. G., Dickens, A. F., Arnarson, T., Nunn, B. L., & Devol, A. H. (2004). What is the oxygen exposure time of laterally transported organic matter along the Washington margin? *Marine Chemistry*, *92*, 157–165.

Keil, R. G., Mayer, L. M., Quay, P. D., Richey, J. E., & Hedges, J. I. (1997). Loss of organic matter from riverine particles in deltas. *Geochimica et Cosmochimica Acta*, *61*, 1507–1511.

Kusch, S., Eglinton, T. I., Mix, A. C., & Mollenhauer, G. (2010). Timescales of lateral sediment transport in the Panama Basin as revealed by radiocarbon ages of alkenones, total organic carbon and foraminifera. *Earth and Planetary Science Letters*, *290*(3), 340–350.

Kusch, S., Kashiyama, Y., Ogawa, N., Altabet, M., Butzin, M., Friedrich, J., et al. (2010). Implications for chloro-and pheopigment synthesis and preservation from combined compound-specific $\delta^{13}C$, $\delta^{15}N$, and $\Delta^{14}C$ analysis. *Biogeosciences*, *7*(12), 4105–4118.

Leithold, E. L., Blair, N. E., & Wegmann, K. W. (2016). Source-to-sink sedimentary systems and global carbon burial: A river runs through it. *Earth-Science Reviews*, *153*, 30–42.

Li, X., Bianchi, T. S., Allison, M. A., Chapman, P., Mitra, S., Zhang, Z., et al. (2012). Composition, abundance and age of total organic carbon in surface sediments from the inner shelf of the East China Sea. *Marine Chemistry*, *145*, 37–52.

Lie, H.-J., & Cho, C.-H. (2016). Seasonal circulation patters of the Yellow and East China Seas derived from satellite-tracked drifter trajectories and hydrographic observations. *Progress in Oceanography*, *146*, 121–141.

Liu, J., Kao, S., Huh, C., & Hung, C. (2013). Gravity flows associated with flood events and carbon burial: Taiwan as instructional source area. *Annual Review of Marine Science*, *5*, 47–68.

Liu, J., Li, A., Xu, K., Velozzi, D., Yang, Z., Milliman, J., & et al. (2006). Sedimentary features of the Yangtze River-derived along-shelf clinoform deposit in the East China Sea. *Continental Shelf Research*, *26*(17), 2141–2156.

Liu, J., Xu, K., Li, A., Milliman, J., Velozzi, D., Xiao, S., & et al. (2007). Flux and fate of Yangtze River sediment delivered to the East China Sea. *Geomorphology*, *85*, 208–224.

Liu, J. P., Milliman, J. D., Gao, S., & Cheng, P. (2004). Holocene development of the Yellow River's subaqueous delta, North Yellow Sea. *Marine Geology*, *209*, 45–67.

Luo, Z., Zhu, J., Wu, H., & Li, X. (2017). Dynamics of the sediment plume over the Yangtze Bank in the Yellow and East China Seas. *Journal of Geophysical Research: Oceans*, *122*, 10,073–10,090. https://doi.org/10.1002/2017JC013215

Marwick, T. R., Tamooh, F., Teodoru, C. R., Borges, A. V., Darchambeau, F., & Bouillon, S. (2015). The age of river-transported carbon: A global perspective. *Global Biogeochemical Cycles*, *29*, 122–137. https://doi.org/10.1002/2014GB004911

Mayer, L. M. (1994). Surface area control of organic carbon accumulation in continental shelf sediments. *Geochimica et Cosmochimica Acta*, *58*, 1271–1284.

McCave, I., & Hall, I. (2006). Size sorting in marine muds: Processes, pitfalls, and prospects for paleoflow-speed proxies. *Geochemistry, Geophysics, Geosystems*, *7*, Q10N05. https://doi.org/10.1029/2006GC001284

McCave, I. N. (1986). Localand globalaspectsof the bottom nephdoid layersin the worldocean. *Netherlands Journal of Sea Research*, *20*, 167–181.

McCave, I. N., Manighetti, B., & Robinson, S. G. (1995). Sortable silt and fine sediment size/compositon slicing: Parameters for palaeocurrent speed and palaeoceanography. *Paleoceanography*, *10*, 593–610. https://doi.org/10.1029/94PA03039

Milliman, J. D., Beardsley, R. C., Yang, Z. S., & Limeburner, R. (1985). Modern Huanghe-derived muds on the outer shelf of the East China Sea: identification and potential transport mechanisms. *Continental Shelf Research*, *4*, 175–188.

Mollenhauer, G., Eglinton, T., Ohkouchi, N., Schneider, R., Müller, P., Grootes, P., & et al. (2003). Asynchronous alkenone and foraminifera records from the Benguela Upwelling System. *Geochimica et Cosmochimica Acta*, *67*(12), 2157–2171.

Mollenhauer, G., & Eglinton, T. I. (2007). Diagenetic and sedimentological controls on the composition of organic matter preserved in California Borderland Basin sediments. *Limnology and Oceanography*, *52*(2), 558–576.

Mollenhauer, G., Eglinton, T. I., Hopmans, E. C., & Damsté, J. S. S. (2008). A radiocarbon-based assessment of the preservation characteristics of crenarchaeol and alkenones from continental margin sediments. *Organic Geochemistry*, *39*(8), 1039–1045.

Mollenhauer, G., Inthorn, M., Vogt, T., Zabel, M., Sinninghe Damsté, J. S., & Eglinton, T. I. (2007). Aging of marine organic matter during cross-shelf lateral transport in the Benguela upwelling system revealed by compound-specific radiocarbon dating. *Geochemistry, Geophysics, Geosystems*, *8*, Q09004. https://doi.org/10.1029/2007GC001603

Mollenhauer, G., Kienast, M., Lamy, F., Meggers, H., Schneider, R. R., Hayes, J. M., & et al. (2005). An evaluation of ^{14}C age relationships between co-occurring foraminifera, alkenones, and total organic carbon in continental margin sediments. *Paleoceanography*, *20*, PA1016. https://doi.org/10.1029/2004PA001103

Mollenhauer, G., Mcmanus, J. F., Benthien, A., Müller, P. J., & Eglinton, T. I. (2006). Rapid lateral particle transport in the Argentine Basin: Molecular ^{14}C and ^{230}Th evidence. *Deep-Sea Research*, *53*(7), 1224–1243.

Muller-Karger, F. E., Varela, R., Thunell, R., Luerssen, R., Hu, C., & Walsh, J. J. (2005). The importance of continental margins in the global carbon cycle. *Geophysical Research Letters*, *32*, L01602. https://doi.org/10.1029/2004GL021346

Nuwer, J. M., & Keil, R. G. (2005). Sedimentary organic matter geochemistry of Clayoquot Sound, Vancouver Island, British Columbia. *Limnology and Oceanography*, *50*, 1119–1128.

Ohkouchi, N., Eglinton, T. I., Keigwin, L. D., & Hayes, J. M. (2002). Spatial and temporal offsets between proxy records in a sediment drift. *Science*, *298*(5596), 1224–1227.

Pawlowicz, R., Beardsley, B., & Lentz, S. (2002). Classical tidal harmonic analysis including error estimates in MATLAB using T Tide. *Computers and Geosciences*, *28*, 929–937.

Pedrosa-Pàmies, R., Sanchez-Vidal, A., Calafat, A., Canals, M., & Duran, R. (2013). Impact of storm-induced remobilization on grain size distribution and organic carbon content in sediments from the Blanes Canyon area, NW Mediterranean Sea. *Progress in Oceanography*, *118*, 122–136.

Qiao, S., Shi, X., Wang, G., Zhou, L., Hu, B., Hu, L., et al. (2017). Sediment accumulation and budget in the Bohai Sea, Yellow Sea and East China Sea. *Marine Geology*, *390*, 270–281.

Saito, Y., Katayama, H., Ikehara, K., Kato, Y., Matsumoto, E., Oguri, K., et al. (1998). Transgressive and highstand systems tracts and post-glacial transgression, the East China Sea. *Sedimentary Geology*, *122*(1), 217–232.

Shah, S. R., Mollenhauer, G., Ohkouchi, N., Eglinton, T. I., & Pearson, A. (2008). Origins of archaeal tetraether lipids in sediments: Insights from radiocarbon analysis. *Geochimica et Cosmochimica Acta*, *72*(18), 4577–4594.

Stuiver, M., & Polach, H. A. (1977). Discussion reporting of ^{14}C data. *Radiocarbon*, *19*(3), 355–363.

Su, C.-C., & Huh, C.-A. (2002). ^{210}Pb, ^{137}Cs and $^{239,240}Pu$ in East China Sea sediments: sources, pathways and budgets of sediments and radionuclides. *Marine Geology*, *183*(1), 163–178.

Tao, S., Eglinton, T. I., Montluçon, D. B., McIntyre, C., & Zhao, M. (2015). Pre-aged soil organic carbon as a major component of the Yellow River suspended load: Regional significance and global relevance. *Earth and Planetary Science Letters*, *414*, 77–86.

Tao, S., Eglinton, T. I., Montluçon, D. B., McIntyre, C., & Zhao, M. (2016). Diverse origins and pre-depositional histories of organic matter in contemporary Chinese marginal sea sediments. *Geochimica et Cosmochimica Acta*, *191*, 70–88.

Tesi, T., Langone, L., Goni, M., Turchetto, M., Miserocchi, S., & Boldrin, A. (2008). Source and composition of organic matter in the Bari canyon (Italy): dense water cascading versus particulate export from the upper ocean. *Deep Sea Research Part I: Oceanographic Research Papers*, *55*(7), 813–831.

Tesi, T., Puig, P., Palanques, A., & Goñi, M. (2010). Lateral advection of organic matter in cascading-dominated submarine canyons. *Progress in Oceanography*, *84*(3), 185–203.

Tesi, T., Semiletov, I., Dudarev, O., Andersson, A., & Gustafsson, Ö. (2016). Matrix association effects on hydrodynamic sorting and degradation of terrestrial organic matter during cross-shelf transport in the Laptev and East Siberian shelf seas. *Journal of Geophysical Research: Biogeosciences*, *121*, 731–752. https://doi.org/10.1002/2015JG003067

Tesi, T., Semiletov, I., Hugelius, G., Dudarev, O., Kuhry, P., & Gustafsson, Ö. (2014). Composition and fate of terrigenous organic matter along the Arctic land–ocean continuum in East Siberia: Insights from biomarkers and carbon isotopes. *Geochimica et Cosmochimica Acta*, *133*, 235–256.

Thomsen, L., & Gust, G. (2000). Sediment erosion thresholds and characteristics of resuspended aggregates on the western European continental margin. *Deep Sea Research Part I: Oceanographic Research Papers*, *47*, 1881–1897.

Thomsen, L., & McCave, I. (2000). Aggregation processes in the benthic boundary layer at the Celtic Sea continental margin. *Deep Sea Research Part I: Oceanographic Research Papers*, *47*(8), 1389–1404.

Wagner, T., Kallweit, W., Talbot, H. M., Mollenhauer, G., Boom, A., & Zabel, M. (2014). Microbial biomarkers support organic carbon transport from methane-rich Amazon wetlands to the shelf and deep sea fan during recent and glacial climate conditions. *Organic Geochemistry*, *67*, 85–98.

Wakeham, S. G., & McNichol, A. P. (2014). Transfer of organic carbon through marine water columns to sediments–insights from stable and radiocarbon isotopes of lipid biomarkers. *Biogeosciences*. https://doi.org/10.5194/bg-11-6895-2014

Wang, H., Bi, N., Saito, Y., Wang, Y., Sun, X., Zhang, J., & et al. (2010). Recent changes in sediment delivery by the Huanghe (Yellow River) to the sea: Causes and environmental implications in its estuary. *Journal of Hydrology*, *391*, 302–313.

Wang, H., Saito, Y., Zhang, Y., Bi, N., Sun, X., & Yang, Z. (2011). Recent changes of sediment flux to the western Pacific Ocean from major rivers in East and Southeast Asia. *Earth-Science Reviews*, *108*, 80–100.

Wang, J., Yao, P., Bianchi, T. S., Li, D., Zhao, B., Cui, X., et al. (2015). The effect of particle density on the sources, distribution, and degradation of sedimentary organic carbon in the Changjiang Estuary and adjacent shelf. *Chemical Geology*, *402*, 52–67.

Wang, Q., Guo, X., & Takeoka, H. (2008). Seasonal variations of the Yellow River plume in the Bohai Sea: A model study. *Journal of Geophysical Research*, *113*, C08046. https://doi.org/10.1029/2007JC004555

Wang, X., Luo, C., Ge, T., Xu, C., & Xue, Y. (2016). Controls on the sources and cycling of dissolved inorganic carbon in the Changjiang and Huanghe River estuaries, China: ^{14}C and ^{13}C Studies. *Limnology and Oceanography*, *61*, 1358–1374.

Wang, X., Ma, H., Li, R., Song, Z., & Wu, J. (2012). Seasonal fluxes and source variation of organic carbon transported by two major Chinese Rivers: The Yellow River and Changjiang (Yangtze) River. *Global Biogeochemical Cycles*, GB2025. https://doi.org/10.1029/2011GB004130

Wu, Y., Eglinton, T. I., Yang, L., Deng, B., Montluçon, D., & Zhang, J. (2013). Spatial variability in the abundance, composition, and age of organic matter in surficial sediments of the East China Sea. *Journal of Geophysical Research: Biogeosciences*, *118*, 1495–1507. https://doi.org/10.1002/2013JG002286

Xu, K., Milliman, J. D., Li, A., Liu, J. P., Kao, S.-J., & Wan, S. (2009). Yangtze-and Taiwan-derived sediments on the inner shelf of East China Sea. *Continental Shelf Research*, *29*(18), 2240–2256.

Yang, S. L., Milliman, J. D., Xu, K. H., Deng, B., Zhang, X. Y., & Luo, X. X. (2014). Downstream sedimentary and geomorphic impacts of the Three Gorges Dam on the Yangtze River. *Earth Science Reviews*, *138*, 409–486.

Yang, S. L., Xu, K. H., Milliman, J. D., Yang, H. F., & Wu, C. S. (2015). Decline of Yangtze River water and sediment discharge: Impact from natural and anthropogenic changes. *Scientific Reports*, *5*, 12,581. https://doi.org/10.1038/srep12581

Yang, Z., Ji, Y., Bi, N., Lei, K., & Wang, H. (2011). Sediment transport off the Huanghe (Yellow River) delta and in the adjacent Bohai Sea in winter and seasonal comparison. *Estuarine, Coastal and Shelf Science*, *93*, 173–181.

Yang, Z., & Liu, J. (2007). A unique Yellow River-derived distal subaqueous delta in the Yellow Sea. *Marine Geology*, *240*, 169–176.

Yao, P., Zhao, B., Bianchi, T. S., Guo, Z., Zhao, M., Li, D., et al. (2014). Remineralization of sedimentary organic carbon in mud deposits of the Changjiang Estuary and adjacent shelf: Implications for carbon preservation and authigenic mineral formation. *Continental Shelf Research*, *91*, 1–11.

Yao, P., Yu, Z., Bianchi, T. S., Guo, Z., Zhao, M., Knappy, C. S., et al. (2015). A multiproxy analysis of sedimentary organic carbon in the Changjiang Estuary and adjacent shelf. *Journal of Geophysical Research: Biogeosciences*, *120*, 1407–1429. https://doi.org/10.1002/2014JG002831

Zhu, Z. Y., Zhang, J., Wu, Y., & Lin, J. (2006). Bulk particulate organic carbon in the East China Sea: Tidal influence and bottom transport. *Progress in Oceanography*, *69*, 37–60.

Zonneveld, K., Versteegh, G., Kasten, S., Eglinton, T. I., Emeis, K.-C., Huguet, C., et al. (2010). Selective preservation of organic matter in marine environments; processes and impact on the sedimentary record. *Biogeosciences*, *7*(2), 483–511.